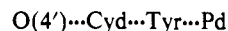


the rings is 15.5°). The closest contacts between the atoms of the rings are 3.49 (1) and 3.41 (1) Å for C(5)···C(15) and C(5)···C(16), respectively. Stacking interactions between purine and pyrimidine bases and tyrosine rings are thought to be of significance for protein-nucleic acid recognition. Studies on crystal structure of the aminoglycosyl antibiotic puromycin containing the *p*-methoxyphenylalanyl ring and the adenine base have shown³² that the bases and the aromatic rings form columns of alternating stacks with an interplanar separation of about 3.4 Å. However, the structures containing both pyrimidine bases and tyrosine residues studied so far exhibit rather different modes of interaction. In the staphylococcal nuclease-thymidine 3',5'-diphosphate-Ca²⁺ complex, the thymine ring and the phenyl ring of Tyr 113 are almost parallel but not stacked with each other.³³ Another pattern is observed in the 1-thyminylacetic acid-tyramine (1:1) complex,³⁴ where the hydroxy group of the tyramine molecule, and not the aromatic ring, is located above the pyrimidine ring. The stacking sequence in the crystal structure of Pd(Gly-L-Tyr)(Cyd) can be described by the scheme



with quite extensive overlapping between the cytidine and tyrosine aromatic rings. As mentioned earlier, the tyrosine residue can interact with nucleosides both in a stacking mode and by formation of hydrogen bonding through its OH group. However, there is no hydrogen-bonding interaction between the hydroxyl group of tyrosine and the nucleoside in the present structure. Instead, the OH group is hydrogen bonded to the carbonyl of the glycine residue, with O(8)···O(9) distance of 2.65 (1) Å. The tyrosine OH group is also involved in the hydrogen bonding (see Table VII) with water of crystallization H₂O(2) and the D···A distance [O(W2)···O(8)] is 2.86 (1) Å.

Acknowledgment. We gratefully thank Professor H. Kozłowski, University of Wrocław, Wrocław, Poland, for very helpful discussions, the National Institutes of Health for a research grant (GM-17378), and the College of Agricultural and Life Sciences of the University of Wisconsin for their continued support.

Registry No. Pd(Gly-L-Tyr)(Cyd), 84132-87-6.

Supplementary Material Available: Tables of thermal parameters and structure factors for all atoms of Pd(Gly-L-Tyr)(Cyd)·6.5H₂O (17 pages). Ordering information is given on any current masthead page.

(32) Sundaralingam, M.; Arora, S. K. *J. Mol. Biol.* **1972**, *71*, 49-70.

(33) Cotton, F. A.; Hazen, E. E.; Legg, M. J. *Proc. Natl. Acad. Sci. U.S.A.* **1979**, *76*, 2551-2555.

(34) Ogawa, K.; Tago, L.; Ishida, T.; Tomita, K.-I. *Acta Crystallogr., Sect. B* **1980**, *B36*, 2095-2099.

The Bicarbonate Proton in Carbonic Anhydrase Catalysis

Y. Pocker* and Thomas L. Deits

Contribution from the Department of Chemistry, BG-10, University of Washington, Seattle, Washington 98195. Received March 1, 1982

Abstract: Substitution of an alkyl group (methyl through *n*-pentyl) for the proton of HCO₃⁻ dramatically alters the properties of the resultant alkyl carbonate esters, ROCO₂⁻, toward bovine carbonic anhydrase (BCA). While HCO₃⁻ is the natural substrate of BCA, with a turnover number of ~10⁶ s⁻¹, the alkyl carbonates show no detectable substrate activity under conditions designed to detect catalysis of substrates with turnover numbers less than 10¹ s⁻¹. The alkyl carbonates bind efficiently to BCA, however, acting as typical anionic inhibitors of BCA-catalyzed CO₂ hydration, with K_i values comparable to those of the alkyl carboxylates, RCO₂⁻, under the same conditions. We hypothesize the substitution of an alkyl group inhibits a proton transfer essential in the BCA-catalyzed dehydration of HCO₃⁻. We further show that the proton of HCO₃⁻ also permits a unique binding interaction with BCA. At high pH (pH 9.0), HCO₃⁻ inhibits BCA-catalyzed CO₂ hydration by a linear mixed noncompetitive mechanism, distinct from the linear uncompetitive mechanism observed for the alkyl carbonates and other anions of diverse structure. We demonstrate the congruence of these results with our previous rapid-equilibrium kinetic analysis of BCA catalysis and offer a molecular mechanism for carbonic anhydrase that provides an appealing physical model for catalysis.

Carbonic anhydrase (CA) is a widely distributed Zn(II) metalloenzyme of exceptional catalytic efficiency.^{1,2} Its physiological activity, the catalysis of the reversible hydration of CO₂ and dehydration of HCO₃⁻, is carried out with turnover numbers approaching 10⁶ s⁻¹. A critical question that remains unanswered in the elucidation of the molecular details of catalysis is the role of the HCO₃⁻ proton in the catalytic cycle.

The net uptake and release of a proton from the enzyme during the course of a complete catalytic cycle are required by the reaction stoichiometry. The function, if any, of the proton of the HCO₃⁻ ion itself in the catalytic cycle is a quite distinct question, which, if understood, could strongly constrain acceptable mechanisms for CA catalysis. To probe this question, we have initiated the first substrate analogue study of the catalysis by CA of HCO₃⁻ dehydration, employing as structural analogues the alkyl carbonates ROCO₂⁻.

We have previously characterized the solution kinetic parameters for alkyl carbonate decomposition under physiological conditions, demonstrating the full congruence of the mechanism of decomposition of the alkyl carbonates and HCO₃⁻ in the absence of CA.³ The alkyl carbonates therefore appear to be excellent structural and mechanistic analogues of HCO₃⁻.

In order to understand the interaction of the alkyl carbonates with carbonic anhydrase, account must be taken of the anionic nature of these compounds. To this end, we have recently completed and reported upon a comprehensive analysis of the inhibition of CA-catalyzed CO₂ hydration by monoanions, the results of which have led us to propose a novel mechanism of catalysis for CA.^{4,5}

From the results of our previous work and the present study, we find, on the basis of the alkyl carbonates as substrate analogues, that the HCO₃⁻ proton is critical in catalytic turnover, and, on the basis of the alkyl carbonates and HCO₃⁻ as inhibitors of

(1) Pocker, Y.; Sarkanen, S. *Adv. Enzymol. Relat. Areas Mol. Biol.* **1978**, *47*, 149.

(2) Wyeth, P.; Prince, R. H. *Inorg. Perspect. Biol. Med.* **1977**, *1*, 37.

(3) Pocker, Y.; Davison, B. L.; Deits, T. L. *J. Am. Chem. Soc.* **1978**, *100*, 3564.

CA-catalyzed CO₂ hydration, that the proton of HCO₃⁻ plays a hitherto unsuspected role in substrate binding. We further demonstrate the congruence of these results with our proposed catalytic mechanism for CA and suggest that a relatively simple rapid-equilibrium analysis of carbonic anhydrase activity can provide considerable physical insight into the molecular steps of CA catalysis.

Experimental Section

Materials. Reagent grade, 1,2-dimethylimidazole and *N*-methylimidazole were distilled under N₂ and stored in dark well-sealed bottles under N₂ at 4 °C. Reagent grade *p*-nitrophenol was purified by sublimation. CO₂ solutions were prepared by bubbling Airco Coleman Grade CO₂ through distilled deionized H₂O thermostated at 30 °C, yielding a CO₂ concentration of 0.030 M. Bovine carbonic anhydrase (BCA) and bovine serum albumin (BSA) (Worthington Biochemicals) were used without further purification. Active enzyme concentration was determined by inhibition studies with the potent inhibitor acetazolamide; the resulting data were plotted by the method of Henderson.^{6a} Alkyl carbonates were synthesized as previously described,³ with the exception that *sec*-butyl alkyl carbonate was prepared as the potassium salt to facilitate formation of the alkoxide prior to CO₂ addition. Other reagents were of the highest grade available.

pH-Stat System. pH-stat kinetics were performed on a Radiometer pH-stat system, consisting of a type TTT1C automatic titrator, type PHA 630T scale expander, type ABU1b auto burette, and a type SBR2a chart recorder. The automatic titrator was modified to incorporate a photoelectric chopper. Reaction temperature was maintained at 25.0 ± 0.1 °C with a circulating water bath.

The reaction cell consisted of a jacketed Kimax 30M fritted-glass filter. The filter neck was bent 90° just below the glass frit to accommodate magnetic stirring of the reaction mixture. H₂O-saturated N₂ gas was bubbled through the filter neck to scrub product CO₂ produced from alkyl carbonate or HCO₃⁻ decomposition, in order to suppress the competing back reaction. In this reaction cell with a 5-mL-sample volume, N₂ scrubbing rates of from 1 to 1.8 L/min were required to efficiently remove product CO₂. Our criterion for efficient scrubbing is independence of the observed rate constant of decomposition of the alkyl carbonate from the flow rate of N₂ gas.

Gas flows of this rate have, however, a tendency to inactivate BCA at concentrations usual in catalytic experiments, ca. 10⁻⁷ M. Treatment of BCA at pH 7 at a flow rate of 1 L/min of N₂ for approximately 90 s prior to reaction initiation with HCO₃⁻ leads to 50% inactivation of the enzyme. Addition of BSA to the reaction cell prevents this inactivation. At a weight ratio of 200 mg of BSA/mg of BCA, negligible activity is lost over times exceeding 10 min. In order to minimize foaming induced by this added protein, a drop of 1-octanol was added to each reaction mixture. In control experiments, added 1-octanol had no effect on alkyl carbonate decomposition or on BCA activity.

HCO₃⁻ decomposition reactions were initiated by injecting a freshly prepared stock solution of HCO₃⁻. For initiation of alkyl carbonate decomposition reactions, an aliquot of alkyl carbonate was weighed into a 20 × 3 mm piece of glass tubing fitted with rubber septa on each end. A portion of the reaction buffer was injected through this chamber from a syringe and simultaneously ejected into the reaction cell via an outlet syringe needle. Phosphate buffers, 0.02 M, maintained at ionic strength 0.1 M with Na₂SO₄ were employed for all pH-stat experiments.

Stopped-Flow System. Initial rate determinations for studies of BCA-catalyzed CO₂ hydration and HCO₃⁻ dehydration were performed on a Durrum-Gibson stopped-flow apparatus, modified in these laboratories. Modifications include interfacing to a PDP 8L computer for data acquisition, permitting real time acquisition of 125 transmittance data points in periods as short as 11 ms. Data from up to 25 kinetic runs can be stored before data reduction commences, considerably facilitating data acquisition. Initial rates are determined by unweighted linear least-squares analysis of the transmittance data, converted to absorbance readings, and plotted against time. A pneumatic electronically controlled drive system has also been incorporated. Drive pressure and duration are under operator control, eliminating artifacts due to release of the drive piston during data collection and enhancing reproducibility of drive motion.

Initial rate determinations were performed by employing the changing pH-indicator method.^{6b} Two buffer-indicator pairs, 1,2-dimethylimidazole (pK_a = 8.22) with *m*-cresol purple (pK_a = 8.43) and *N*-

methylimidazole (pK_a = 7.19) with *p*-nitrophenol (pK_a = 7.07), were employed. Buffer concentration in the reaction cell was maintained at 0.02 M in all experiments. Ionic strength was maintained at 0.2 with Na₂SO₄. In those inhibition experiments where the concentration of added inhibitory anion would significantly (greater than 5%) perturb the total ionic strength, the concentration of added Na₂SO₄ was adjusted to compensate. Indicator concentrations were chosen at each pH to give an initial absorbance of 0.3–0.4 for optimal photomultiplier response yielding indicator concentrations near 10⁻⁵ M, varying somewhat with pH.

Buffer factors^{6b} were determined experimentally by titration at one pH value for each buffer-indicator pair and found to agree well with buffer factors (*Q*) calculated by the formula⁵

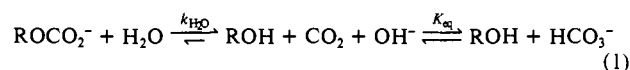
$$Q_{\text{calcd}} = \frac{[\text{Buff}]}{[\text{In}]L\Delta\epsilon} \left(\frac{K_a^{\text{Buff}}}{K_a^{\text{In}}} \right) \left(\frac{K_a^{\text{In}} + [\text{H}^+]}{K_a^{\text{Buff}} + [\text{H}^+]} \right)^2$$

[Buff] and [In] represent total buffer and indicator concentrations, respectively, and K_a^{Buff} and K_a^{In} buffer and indicator ionization constants. Δε is the difference in molar extinction coefficient between the acidic and basic forms of the indicator, and L is the reaction-cell optical path length in cm. For *m*-cresol purple, Δε = 3.2 × 10⁴; for *p*-nitrophenol, Δε = 1.9 × 10⁴ at 578 and 400 nm, respectively.

CO₂ and HCO₃⁻ solutions were prepared as previously described.⁵ Substrate concentrations employed ranged from 0.015 to 0.0025 M for CO₂ and from 0.06 to 0.006 M for HCO₃⁻. Enzyme concentration was adjusted to give velocities at least 10-fold larger than the uncatalyzed rates of reaction, typically 1–3 × 10⁻⁷ M. All kinetic data were collected at 25 ± 0.01 °C. In most kinetic runs, with exceptions noted below, a 3–5-ms delay following solution mixing was programmed to eliminate mixing artifacts. Initial rate data were taken for 15–20 ms following the mixing delay. Kinetic data were analyzed as previously described.⁵

In stopped-flow studies of HCO₃⁻ inhibition of BCA-catalyzed CO₂ hydration, enzyme, buffer, and HCO₃⁻ were placed in one syringe of the stopped-flow apparatus, and a freshly prepared stock solution of CO₂ was placed in the other syringe. For the analysis of alkyl carbonate inhibition, an aliquot of dry alkyl carbonate was weighed into an oven-dried volumetric flask. The volumetric flask was quickly filled with enzyme–buffer stock solution and rapidly mixed. The solution was transferred to a stopped-flow syringe, and kinetic data were collected at a rate of approximately one kinetic run every 1.5 s. When this scheme is used, 10 replicate kinetic runs could be completed within 40 s after the initial contact of alkyl carbonate and buffer. Under these conditions, based on the spontaneous rates of alkyl carbonate decomposition³ at pH 9, less than 3% of the alkyl carbonate will have decomposed to HCO₃⁻ while kinetic data are taken.

In experiments designed to detect substrate activity of the alkyl carbonates by stopped-flow techniques, alkyl carbonates were mixed with H₂O rather than buffer by the methods outlined above and then allowed to decompose spontaneously in the stopped-flow syringe by reaction 1.



Given the vast molar excess of H₂O over ROH in the syringe, the added alkyl carbonate will convert to essentially pure HCO₃⁻ with time. The rate of this conversion will be the rate of spontaneous decomposition of the alkyl carbonate, k_{H₂O}.³ In this fashion, mixtures of ROCO₂⁻ and HCO₃⁻ of varying molar ratios can be created in one syringe of the stopped-flow apparatus and then probed for their kinetic properties by rapidly mixing aliquots at intervals with the contents of the other stopped-flow syringe containing buffer at the desired final pH. Since no net proton uptake or release occurs in the decomposition reaction, the assay pH remains constant in all runs.

Results

A. Alkyl Carbonate Substrate Activity. 1. pH-Stat Technique. When the BSA-stabilized pH-stat system was used (see Experimental Section), the initial velocities for ethyl and *sec*-butyl carbonate decomposition were determined as a function of BCA concentration. The initial velocities obtained deviated less than 10% from the velocity measured in the absence of enzyme, even at concentrations of BCA as high as 6 × 10⁻⁵ M. An upper limit on the catalytic activity of BCA toward the alkyl carbonates can be used to place this result in perspective. The apparent first-order rate constant for BCA-catalyzed HCO₃⁻ dehydration, k_{cat}, is 3.9 × 10⁶ s⁻¹. In the current study, if enzyme was saturated with alkyl carbonate under the conditions of assay, k_{cat} for the alkyl carbonates would be the difference between the velocities determined

(4) Pocker, Y.; Deits, T. L. *J. Am. Chem. Soc.* **1981**, *103*, 3949.

(5) Pocker, Y.; Deits, T. L. *J. Am. Chem. Soc.* **1982**, *104*, 2424.

(6) (a) Henderson, P. J. F. *Biochem. J.* **1972**, *127*, 321. (b) Khalifah, R. G. *J. Biol. Chem.* **1971**, *246*, 2561.

with and without enzyme, divided by enzyme concentration. Making the quite liberal assumption that experimental error had hidden a 20% increase in the observed initial velocity at the highest BCA concentration tested would place an upper limit on the enzymatic portion of V_{obsd} of $9 \times 10^{-6} \text{ M s}^{-1}$.

Making the further liberal assumption that the alkyl carbonates have K_m values tenfold higher than the K_m for HCO_3^- would mean that our experiments were carried out at 1% saturation of BCA with substrate. Under this assumption, V_{max} for the alkyl carbonates must be less than $9 \times 10^{-4} \text{ M s}^{-1}$. Dividing this value for V_{max} by enzyme concentration yields an upper limit for k_{cat} for the alkyl carbonates; $k_{\text{cat}} = (9 \times 10^{-4} \text{ M s}^{-1}) / (6 \times 10^{-5} \text{ M}) = 1.4 \times 10^1 \text{ s}^{-1}$. The ratio of k_{cat} for HCO_3^- to the upper limit on k_{cat} for the alkyl carbonates is therefore $(3.9 \times 10^6) / (1.4 \times 10^1) = 1.5 \times 10^5$; thus catalysis of alkyl carbonate decomposition by BCA is at least 5 orders of magnitude less efficient than catalysis of HCO_3^- dehydration under comparable conditions. Since the experimental error is likely to be considerably less than 20%, the relative efficiency of the catalysis of alkyl carbonate decomposition by BCA certainly will not exceed this estimate and in all probability will be considerably weaker.

2. Stopped-Flow Techniques. Two stopped-flow techniques were used to confirm this finding. As discussed in the Experimental Section, it is possible to allow a sample of alkyl carbonate to decompose in one syringe of the stopped-flow apparatus to form HCO_3^- and then probe the activity of the resulting alkyl carbonate/ HCO_3^- mixture by a subsequent rapid mixing experiment at the desired assay pH. Ethyl carbonate was dissolved at $t = 0$ in a stopped-flow syringe and run vs. BCA in pH 6.6 buffer at timed intervals. Ethyl carbonate concentration was initially $5 \times 10^{-3} \text{ M}$ to ensure that HCO_3^- concentration would remain below its K_m value for the course of the experiment. Under these conditions, if the alkyl carbonates have no substrate activity, the only increase in initial velocity with time will be due to the slow conversion of the alkyl carbonate solution in the substrate syringe to HCO_3^- . The rate of change of the initial velocity observed for this experiment is shown in Figure 1a. The initial velocity clearly follows a first-order increase with time, as expected from eq 1. Plots of $\ln [(dA/dt)_\infty - (dA/dt)]$ vs. time were linear, with an average rate constant in replicate determinations of $7.4 \times 10^{-4} \text{ s}^{-1}$, in excellent agreement with the value of $k_{\text{H}_2\text{O}}$ for ethyl carbonate, $8 \times 10^{-4} \text{ s}^{-1}$, determined in pH-stat experiments.³

A second series of experiments using the stopped-flow apparatus confirms this result. In the presence of much higher BCA concentrations than in the previous experiment the criterion for initial rate kinetics, that the initial concentration of substrate (HCO_3^-) must change by less than 5% over the course of the mixing and observation times of the stopped-flow experiment, no longer is obeyed. Indeed, at sufficiently high BCA concentrations and with a slightly longer mixing time (20 ms instead of the usual 10 ms), HCO_3^- can be entirely converted to its equilibrium concentration before observation of dA/dt commences. Under such conditions, the difference in absorbance reading of indicator present after equilibration compared to the absorbance reading at $t = 0$ will be a measure of the concentration of HCO_3^- present.

Our stopped-flow control program automatically reports the initial absorbance (IA) of the reaction solution as measured at the beginning of the observation period. Thus, in the same fashion as the previous experiment, plots of $\ln (\text{IA}_\infty - \text{IA})$ vs. time should also mirror the increase in the concentration of HCO_3^- generated from alkyl carbonate decomposition. At the same time, the initial rate measured in the same experiment after HCO_3^- equilibrates in the spectrophotometer cell should reflect any catalysis due to alkyl carbonate interacting with BCA as a substrate.

Figure 1b shows both the expected first-order increase in initial absorbance measured as a function of time after dissolving of alkyl carbonate and the complete lack of measurable catalysis of residual ethyl carbonate, indicated by the negligible dA/dt value over the course of the experiment. In this experiment, substrate concentration must also be kept low, so that the absorbance change induced by HCO_3^- formed remains within the range over which the indicator buffer factor is constant.^{6b} The rate constant for

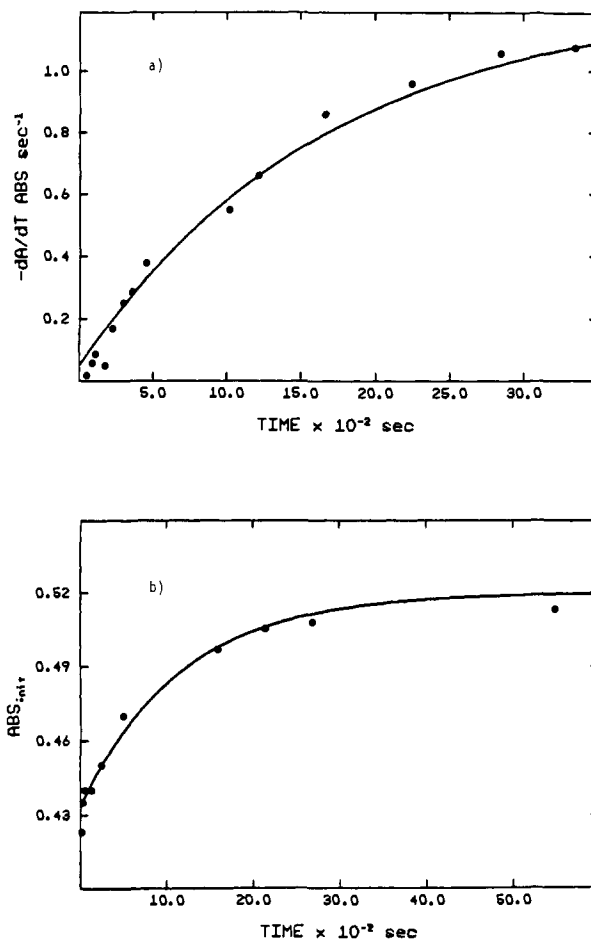


Figure 1. (a) Increase in dA/dt with time as an aqueous solution of $\text{CH}_3\text{CH}_2\text{OCO}_2^-$ decomposes in the stopped-flow syringe. $[\text{CH}_3\text{CH}_2\text{OCO}_2^-] = 4.65 \times 10^{-3} \text{ M}$, $[\text{BCA}] = 2.71 \times 10^{-7} \text{ M}$. Velocity observed with this concentration of BCA and the same molar concentration of HCO_3^- substituted for $\text{CH}_3\text{CH}_2\text{OCO}_2^-$ is 1.5 A/s . Initial absorbance as measured at each time point is 0.475 ± 0.003 . The line is the theoretical first-order curve with $k = 7.4 \times 10^{-4} \text{ s}^{-1}$. (b) Increase in initial absorbance of stopped-flow kinetics runs as an aqueous solution of $\text{CH}_3\text{C}-\text{H}_2\text{OCO}_2^-$ decomposes in the stopped-flow syringe. Average dA/dt value measured at each time point is $0.025 \pm 0.01 \text{ A/s}$, a value not significantly different from the observed velocity of decomposition of $\text{CH}_3\text{CH}_2\text{OCO}_2^-$ measured in the absence of BCA under the same conditions. The line is the theoretical first-order curve with $k = 7.4 \times 10^{-4} \text{ s}^{-1}$.

the change in IA with time measured in replicate experiments is $7.5 \times 10^{-4} \text{ s}^{-1}$, again in excellent agreement with $k_{\text{H}_2\text{O}}$ for ethyl carbonate.³

The above stopped-flow experiments were performed at pH 6.6 where catalysis of alkyl carbonate decomposition by BCA should, by analogy with HCO_3^- , be highly efficient. Repetition of the experiments at pH 7.0, to detect catalysis by the basic form of the enzyme showed the same lack of catalytic activity of BCA toward the alkyl carbonates.

B. Inhibition of BCA-Catalyzed CO_2 Hydration by ROCO_2^- . A conceivable explanation for the lack of catalytic activity of BCA toward the alkyl carbonates would be that no interaction between the enzyme and the substrate analogue occurs. If, for some reason, the steric constraints on HCO_3^- binding and turnover were far stricter than on the hydration reaction, in which a variety of functionalities can be accommodated,¹ then the alkyl carbonates might be excluded from the active site, eliminating any possibility for catalytic interaction. Alternatively, the above experiments might not detect alkyl carbonate substrate activity if the K_m values for the alkyl carbonates were significantly higher than the substrate concentrations employed in the stopped-flow or pH-stat experiments.

To investigate this possibility requires the exploitation of the anionic nature of the alkyl carbonates. Anions of diverse structure

Table I. Kinetic K_i Values for the Inhibition of BCA Catalysis by Alkyl Carbonates (ROCO_2^-) and Alkyl Carboxylates (RCO_2^-)

substrate	CO_2	CO_2	HCO_3^-
pH	9.00	9.00	6.60
inhibitor	ROCO_2^-	RCO_2^-	ROCO_2^-
R	$K_i^{\text{int } a,b}, \text{M}$	$K_i^{\text{int } a,c}, \text{M}$	I_{50}^d, M
H	0.10	0.024	
CH_3	0.079	0.104	0.08
CH_3CH_2	0.120	0.140	0.10
$\text{CH}_3(\text{CH}_2)_2$	0.200	0.128	0.09
$\text{CH}_3(\text{CH}_2)_3$	0.079	0.056	0.05
$\text{CH}_3(\text{CH}_2)_4$	0.025	0.032	0.02

^a K_i values were determined from full Lineweaver-Burk plots comparable to Figure 2, in which at least four inhibitor concentrations were tested at a minimum of four different substrate concentrations. For each pair of substrate and inhibitor concentrations, 15–20 replicate runs were performed. ^b K_i^{int} values are determined from secondary replots of ordinate intercepts⁹ of Lineweaver-Burk plots similar to those of Figure 2. ^c Data from ref 5. ^d I_{50} values represent velocity measurements taken in the presence of at least five inhibitor concentrations at a single substrate concentration, 0.03M; 15–20 replicate runs were performed at each concentration.

inhibit BCA-catalyzed CO_2 hydration at all pH values.⁵ If the alkyl carbonates similarly inhibit BCA, then their interaction with the active site of BCA would be confirmed, and the lack of substrate activity of the alkyl carbonates must reside elsewhere than in active-site binding.

A major obstacle to the analysis of alkyl carbonate interaction by inhibitor studies is the decomposition to HCO_3^- that ensues as soon as the alkyl carbonate is dissolved in H_2O . HCO_3^- is itself an inhibitor of CO_2 hydration⁷ and so would be expected to contribute or might even dominate inhibition in solutions of alkyl carbonates. Techniques to obviate this problem are described above in the Experimental Section.

The alkyl carbonates are indeed inhibitors of BCA-catalyzed CO_2 hydration. Figure 2 shows the pattern of inhibition observed for ethyl and pentyl carbonates, typical of all alkyl carbonates tested. The pattern is clearly uncompetitive, consistent with that for other anions under these conditions, as recently reported.⁵ Table I lists the K_i values determined for bicarbonate and the alkyl carbonates derived from C_1 through C_5 primary aliphatic alcohols.

C. Inhibition of BCA-Catalyzed HCO_3^- Dehydration by ROCO_2^- . Because of the requirement that the alkyl carbonate be dissolved in the buffer stock solution, studies of the inhibition of BCA-catalyzed CO_2 hydration at lower pH values are impossible with the available apparatus. In less basic buffers, acid catalysis of alkyl carbonate decomposition would create unacceptably high HCO_3^- concentrations before rates could be run.

However, an estimate of the inhibitory power of the alkyl carbonates toward BCA-catalyzed HCO_3^- dehydration at low pH can be obtained. Results can be obtained for the alkyl carbonates under conditions comparable to other HCO_3^- inhibition experiments by mixing the solid alkyl carbonate with the HCO_3^- substrate solution, whose equilibrium pH will be near pH 9, and by running kinetics vs. pH 6.6 buffer-enzyme stock solution as fast as possible.

In the preceding analysis of the inhibition of BCA-catalyzed CO_2 hydration at high pH by the alkyl carbonates, the traces of contaminating HCO_3^- formed during the course of analysis will act only as a minor additional inhibitor, with negligible effect on the mechanism or magnitude of alkyl carbonate inhibition. In the analysis of the inhibition of BCA-catalyzed HCO_3^- dehydration by the alkyl carbonates, however, even a trace of HCO_3^- will significantly affect the observed mechanism of inhibition, as its effect will be directly on the $1/[\text{HCO}_3^-]$ axis of the Lineweaver-Burk plot. For this reason, no attempt to make mechanistic deductions or to gain more than an estimate of the inhibitory power of the alkyl carbonates as inhibitors of BCA-catalyzed HCO_3^-

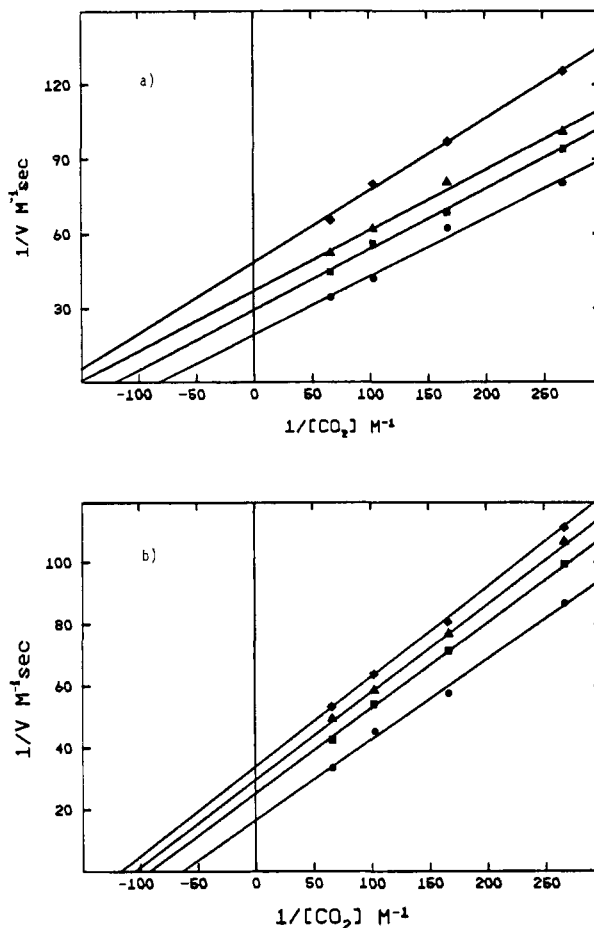


Figure 2. (a) Inhibition of BCA-catalyzed CO_2 hydration by $\text{CH}_3\text{CH}_2\text{H}_2\text{OCO}_2^-$, pH 9.00. $[\text{CH}_3\text{CH}_2\text{OCO}_2^-] = 0$ (\bullet), 5.3×10^{-2} M (\blacksquare), 8.9×10^{-2} M (\blacktriangle), 1.75×10^{-1} M (\blacklozenge). (b) Inhibition of BCA-catalyzed CO_2 hydration by $\text{CH}_3(\text{CH}_2)_4\text{OCO}_2^-$, pH 9.00. $[\text{CH}_3(\text{CH}_2)_4\text{OCO}_2^-] = 0$ (\bullet), 1.3×10^{-2} M (\blacksquare), 1.95×10^{-2} M (\blacktriangle), 2.6×10^{-2} M (\blacklozenge).

dehydration has been made. Table I lists such estimates, taken at a single HCO_3^- concentration, 0.03 M, and expressed as I_{50} values, i.e., the concentration of inhibitor required to reduce the enzymatic velocity by 50%. Despite the approximate nature of these data, the magnitude of the I_{50} values is in reasonable accord with the more accurate data taken at pH 9.0 (Table I). As expected for typical anionic inhibitors of BCA,⁵ the alkyl carbonates appear to inhibit slightly more effectively at low pH, while retaining the same relative order of binding potency at the two pH values tested.

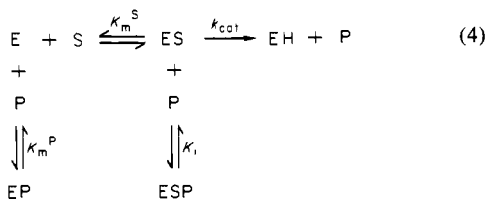
D. Inhibition of BCA-Catalyzed CO_2 Hydration by HCO_3^- . For comparative purposes, the inhibition of BCA-catalyzed CO_2 hydration by HCO_3^- was also determined. Equilibrium solutions of HCO_3^- at pH 9.0 are predominantly composed of HCO_3^- , permitting treatment of HCO_3^- as a simple anion in kinetic studies of inhibition of BCA-catalyzed CO_2 hydration.

Figure 3 represents the results of such an experiment. The pattern of inhibition observed is best described as linear non-competitive. This pattern is unique among anions tested at this pH, both in this study of inhibition by the alkyl carbonates and in our previous study of inhibition of BCA by 13 anions of diverse structure.⁵ The implications of this result will be discussed below.

E. Inhibition of BCA-Catalyzed CO_2 Hydration by Alcohols. A side product of the decomposition of the alkyl carbonates is the corresponding alcohol. Any inhibitory effect of the alcohol so formed must be taken into account in the analysis of alkyl carbonate interactions as substrate or inhibitor. At the concentrations of alkyl carbonates employed, the alcohol concentration will not exceed 0.02 M at any time during the course of these experiments. C_1 – C_5 primary alcohols were therefore tested for inhibitory power toward BCA-catalyzed CO_2 hydration at pH 9.0 at concentrations

(7) Steiner, H.; Jonsson, B.-H.; Lindskog, S. *FEBS Lett.* 1976, 62, 16.

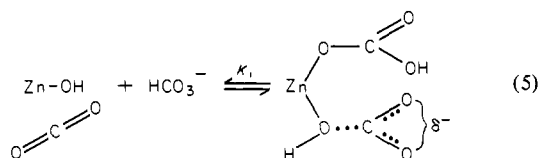
D. The HCO_3^- Proton in Inhibition. As discussed above, the inhibition of BCA-catalyzed CO_2 hydration at high pH by the alkyl carbonates follows the same uncompetitive pattern exhibited by all other simple anions. The same formal scheme proposed to account for this phenomenon is quantitatively consistent with the inhibition of BCA-catalyzed CO_2 hydration by HCO_3^- at high pH. According to this model, HCO_3^- should deplete the available concentration of active enzyme by binding in two modes: as an alternate substrate with a dissociation constant equal to the kinetic K_m value for HCO_3^- and as an inhibitory anion with a binding constant, K_i , comparable to that of structurally similar anions. These equilibria may be depicted as in eq 4.



A rapid-equilibrium analysis⁹ of eq 4 shows that the apparent K_i value derived from a replot of the ordinate intercepts of Figure 3 will determine the K_i value of eq 4, and the apparent K_i value derived from slope replots of Figure 3 should measure K_m^P of eq 4. K_m^P can be independently determined; from kinetic studies^{10,11} its value is 0.035 M. The intercept replot derived K_i value can be reasonably expected to be comparable to that of other structurally similar anions, for example, CH_3CO_2^- , which has a K_i value of 0.1 M under the same conditions. The observed values from Figure 3 are respectively, $K_m^P = 0.04$ and $K_i = 0.10$ M, in excellent agreement with the predictions of the model.

E. The HCO_3^- Proton in Substrate Binding. The unique pattern of inhibition of BCA-catalyzed CO_2 hydration by HCO_3^- is thereby explained by an effect on the slope of the Lineweaver-Burk plot caused by HCO_3^- binding $\text{Zn}^{\text{II}}\text{-OH}$ in the absence of CO_2 , a mode of anion binding denied to other anions tested, including the alkyl carbonates.

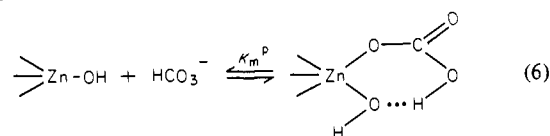
The structure of the two bound forms of HCO_3^- can be described in terms of our previously presented model for CA catalysis and inhibition. The species responsible for the change in the Lineweaver-Burk ordinate intercept with increasing HCO_3^- concentration is given in eq 5.



This species is in strict analogy to that proposed for the uncompetitive binding mode observed for other monoanions at high pH (eq 3).

The effect of HCO_3^- on the slope of Lineweaver-Burke inhibition plots, labeled K_m^P in eq 4, is unique to HCO_3^- among anions tested in this and our previous study and indicates that HCO_3^- can interact as an inhibitor with CA at high pH in the absence of substrate. If, as we propose, the kinetically determined K_m value for HCO_3^- is indeed a substrate dissociation constant, how can its pH independence be accounted for in view of the evident pH dependence of the binding of other anions? We have rationalized binding of other anions at high pH to CA in the presence of CO_2 by proposing a Lewis acid interaction of CO_2 with $\text{Zn}^{\text{II}}\text{-OH}$, which reduces the electron density on $\text{Zn}(\text{II})$.³ HCO_3^- has the capacity to function in a similar fashion, mediating its own binding by a Brønsted acid interaction, by means of the

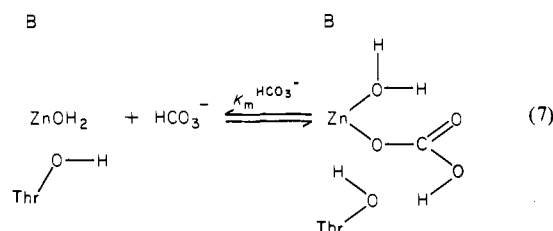
HCO_3^- proton as given in eq 6.



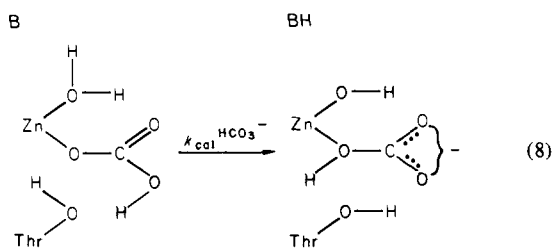
Such a proposal is consistent with the absence of a significant K_i^{slope} term in the inhibitory patterns of alkyl carbonates and other anions lacking a suitable acidic proton. Of course, such a binding mode must be nonproductive to be consistent with the kinetics of CA-catalyzed HCO_3^- dehydration. The proposed mode of binding of HCO_3^- to $\text{Zn}^{\text{II}}\text{-OH}$ should reasonably apply more generally to other anions that have exchangeable protons of similar $\text{p}K_a$ appropriately juxtaposed. Our proposal is, in fact, analogous to a recent proposal^{1,12} for the binding to the CA active site of aromatic sulfonamides, nitrogen acids with $\text{p}K_a$ values close to that of HCO_3^- , and extremely potent inhibitors of CA.

The product inhibition of BCA-catalyzed CO_2 hydration has been previously investigated, with quantitatively similar results.⁷ The previous authors attributed the presence of an $[\text{S}][\text{P}]$ term, equivalent to the K_i term of eq 5, in the kinetic analysis of HCO_3^- inhibition as a consequence of a rate-limiting intramolecular proton transfer in the catalytic cycle. In such an interpretation, no enzyme species contains both bound CO_2 and HCO_3^- ; the $[\text{S}][\text{P}]$ term is only an apparent binding term. Under our interpretation, a species containing both bound CO_2 and HCO_3^- is in fact physically present. Furthermore, under our analysis, both apparent binding constants, K_i and K_m^P for HCO_3^- inhibition, are quantitatively predicted from other data on CA catalysis of CO_2 hydration and HCO_3^- dehydration.

F. The HCO_3^- Proton in CA Catalysis. Our previously proposed molecular mechanism of CA catalysis is consistent with the observations on the alkyl carbonates presented above and was in fact designed with these results as an important kinetic criterion. In accordance with our proposal, HCO_3^- binds productively to the low pH form of CA in the same fashion as other anions. Our depiction of further steps in the catalytic cycle involves two conserved active-site residues: a nonligand histidine near the $\text{Zn}(\text{II})$ ion, and a threonine apparently H bonded to the $\text{Zn}(\text{II})$ oxygen ligand in the X-ray crystal structure. The initial HCO_3^- binding step, then, can be represented as follows (here B represents the active-site histidine, as well as any additional intervening H_2O molecules that may participate):



The alkyl carbonates bind in the same fashion, consistent with the numerical similarity of their K_i values to those of the alkyl carboxylates and to the K_m value for HCO_3^- . The critical catalytic step denied the alkyl carbonates is a subsequent proton transfer, involving both active site residues and mediated by $\text{Zn}(\text{II})$.



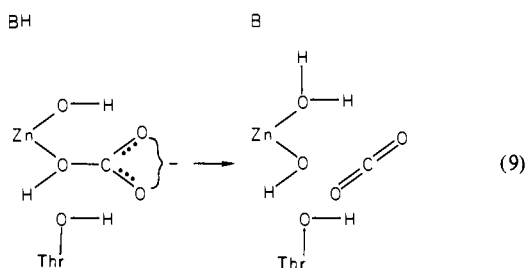
(9) Segel, I. H. "Enzyme Kinetics"; Wiley-Interscience: New York, 1975; pp 170-178.

(10) Pocker, Y.; Bjorkquist, D. W. *Biochemistry* 1977, 16, 5698.

(11) Pocker, Y.; Deits, T. L.; Tanaka, N. In "Advances in Solution Chemistry"; Bertini, I., Lunazzi, L., Dei, A., Eds.; Plenum, New York, 1981; pp 253-274.

(12) Sarkanen, S. "The Oxonase and Esterase Activities of Carbonic Anhydrase: Kinetic and Mechanistic Studies", Ph.D. Thesis, University of Washington, Seattle, WA, 1976.

C-O bond breaking at this stage would convert HCO_3^- to CO_2 but would leave an unstable $\text{Zn}^{\text{II}}(\text{OH})_2$ complex in the active site. Reprotonation of the $\text{Zn}^{\text{II}}\text{-OH}$ ligand by BH, coincident with C-O bond breaking, avoids the formation of such highly basic transition state structures.



The enzyme is now in its basic form, as required by the reaction stoichiometry. A proton-transfer step, to reprotonate the enzyme from external medium, and loss of H_2O from $\text{Zn}(\text{II})$ complete the HCO_3^- catalytic cycle. The importance of proton-transfer steps in our suggested mechanism is clear. The active site of CA is structurally rather open; the alkyl carbonates, alkyl carboxylates, and HCO_3^- bind to and inhibit CA with internally consistent, comparable K_i values (see above). Yet the alkyl carbonates, despite a degree of interaction in the active site comparable to that of HCO_3^- , exhibit no detectable substrate activity. The possibility that strict steric restraints on the positioning of HCO_3^- vs. the alkyl carbonates in the active site might determine substrate activity has no support in the literature of CA; alternate substrates of great variation in structure are accommodated in catalysis,¹ and anions of diverse structure inhibit CA with K_i values generally uncorrelated with anion size.^{1,5} These strongly suggest an essential role for the HCO_3^- proton in CA catalysis.

Conclusion

We have shown in our previous study that a simple rapid equilibrium analysis accounts quantitatively for the anionic inhibition of BCA-catalyzed CO_2 hydration and HCO_3^- dehydration over the full range of enzyme catalytic activity. In the present study we further demonstrate that the inhibition of BCA-catalyzed CO_2 hydration by HCO_3^- can also be quantitatively analyzed by the same rapid equilibrium scheme. The complete absence of

catalysis of alkyl carbonate decomposition by BCA and the demonstration of a distinct inhibitory pattern for HCO_3^- strengthen the assertion that the proton of HCO_3^- performs a critical function in substrate binding and turnover.

This simplified analysis leads us to suggest that kinetic K_m values for CO_2 and HCO_3^- might in fact represent substrate dissociation constants. While a pH-independent substrate dissociation constant for CO_2 , an uncharged species, is not unreasonable, a pH-independent substrate dissociation constant for HCO_3^- seemed heretofore to fly in the face of a substantial literature documenting the pH dependence of anion binding determined by both physical and kinetic techniques. Given, however, our recent observation⁵ that the binding affinity of anions to the $\text{BCA}\text{-CO}_2$ complex changes only by a factor of 2 between pH 6 and 9, a pH-independent binding affinity for HCO_3^- became a considerably more reasonable possibility. We feel that the identification of pH-independent K_m values for CO_2 and HCO_3^- determined in kinetic experiments with substrate dissociation constants as demanded by a simple analysis of CA catalytic parameters should be entertained as an important conceptual simplification.

The results we have presented above and the mechanism we propose present an appealing structural model for the mechanism of CA catalysis. The implications of these structures lead to fruitful mechanistic insights into a number of diverse observations on this fascinating catalyst. We believe that our suggestions may provide some guidance in the search for a molecular mechanism for carbonic anhydrase catalysis.

Acknowledgment. We are grateful to the National Science Foundation and the National Institutes of Health for partial support of this research. T. L. Deits acknowledges the support of the Chevron Corporation for a predoctoral fellowship during the course of this research and the American Cancer Society for a postdoctoral fellowship during the preparation of this manuscript. We thank Drs. Conrad T. O. Fong, Robert R. Miksch, Kenneth W. Raymond, and Simo Sarkanen for valuable discussions and Donald B. Moore for his diligent assistance with computer interfacing.

Registry No. CA, 9001-03-0; HCO_3^- , 71-52-3; CO_2 , 124-38-9; HOC-O_2^- , 71-52-3; $\text{CH}_3\text{OCO}_2^-$, 49745-25-7; $\text{CH}_3\text{CH}_2\text{OCO}_2^-$, 49745-26-8; $\text{CH}_3(\text{CH}_2)_2\text{OCO}_2^-$, 84073-84-7; $\text{CH}_3(\text{CH}_2)_3\text{OCO}_2^-$, 44746-83-0; $\text{CH}_3(\text{CH}_2)_4\text{OCO}_2^-$, 84073-85-8.

Flexibility of Nucleic Acid Conformations. 1. Comparison of the Intensities of the Raman-Active Backbone Vibrations in Double-Helical Nucleic Acids and Model Double-Helical Dinucleotides Crystals

Gerald A. Thomas and Warner L. Peticolas*

Contribution from the Department of Chemistry and Institute of Molecular Biology, University of Oregon, Eugene, Oregon 97403. Received April 5, 1982

Abstract: Raman spectroscopic measurements have been made on crystals of three dinucleotides whose sugar-phosphate conformation is precisely known from X-ray diffraction measurements. These are uridylyl(3'-5')adenosine monophosphate (UpA), guanylyl(3'-5')cytidine nonahydrate (GpC), and sodium thymidylyl(5'-3')thymidylate 5'-hydrate (pTpT). The first two dinucleotides belong to the A-genus conformation with a C3'-endo ribose ring pucker and exhibit the typical frequency and intensity of the A-genus Raman marker band. On the other hand pTpT belongs to the B genus (C2'-endo furanose ring conformation). For this latter crystal, the conformationally dependent B-genus Raman marker band at 833 cm^{-1} is much more intense than that found in ordinary B-DNA in fibers or in solutions. These results are discussed with references to recent potential energy calculations. It is suggested that the deoxyribose rings in B-DNA are less rigid than in either A-DNA or ordered RNA. Some flexibility of the furanose rings is suggested to be responsible for the complete absence of either C2'- or C3'-endo marker bands for the dinucleotides in solution at room temperature.

Earlier work in this laboratory on the correlations that exist between the X-ray determined conformation and the Raman

spectra of fibers of deoxyribonucleic acid clearly show the existence of certain Raman bands that are indicative of the A, B, and C